THE INFLUENCE OF ASPECTRATIO ON THE MECHANICAL PROPERTIES OF MEDIUM AND LONG COLUMNS OF LAND T-SHAPED CONCRETE FILLED STEEL TUBULAR

Li Wen, Gu Changlin, Zhang Weidao
Northeast Petroleum University, Daqing, Heilongjiang 1633128, China
Email: 2571056859@qq.com

ABSTRACT: *In order to study the influence law of aspect ratio on the mechanical properties of medium and long columns of L and T-shaped concrete filled steel tube (CFST), the finite element software ABAQUS is used to simulate the members with different aspect ratio through the designed contrast test. The analysis results of experimental data show that the critical load of L and T-shaped specimens increases exponentially with the decrease of aspect ratio. The influence of aspect ratio on the bearing capacity of L and T-shaped CFST columns is very important. With the increase of aspect ratio, the curve growth rate of the specimen in the elastic deformation stage becomes lower and lower, and the displacement of specimen reaching the critical load decreases gradually. At the same time, the ductility of the specimen will increase, while the risk of instability and failure of L and T-shaped CFST will also increase sharply. Therefore, it is concluded that the analysis of the influence of aspect ratio on the mechanical properties of CFST columns should be strengthened.*

KEY WORDS*: Concrete filled steel tube; Aspect ratio; Critical load; Bearing capacity; Ductility*

1 INTRODUCTION

Special-shaped column is the general term of special-shaped section columns. Its representative T and L-shaped section forms can meet the requirements for building height, spatial layout and aesthetic individuality. Because of the combination of high bearing capacity, good deformation capacity and seismic performance of steel as well as the fire resistance and stability performance of concrete, concrete filled steel tube (CFST) structureis more and more popular in the construction industry. The special-shaped concrete-filled steel tubular column not only combines the bearing capacity and deformation capacity of super-high steel tube, but also combines the durability, stability and fire resistance of concrete, thus the systematic study of L and T-shaped components has become a very necessary subject at present (Wang and Lv, 2005; Wang, 2005; Lu et al., 2007). In (Uy, B., 2000 and 2001) further studied the axial compression, biaxial compression and compression bending performance of concrete-filled square steel tube specimens. After comparing the test data with the European code values, the formula was modified to try to get a more practical solution, which provided a theoretical basis for architectural structure design. In (Shanmugam N. E. et al, 2002) obtained the criterion of steel tube buckling by studying the concrete-filled square steel tube, and obtained the formula of ultimate bearing capacity of the specimen under axial compression by using the "width theory". After (Hu H T, et al ,2003) used ABAQUS finite element software to study the constraint effect of steel tube wall thickness on the core concrete, and preliminarily obtained the influence rule of three-dimensional constraint on the constitutive behavior of steel tube and concrete. In (Rong and Chen, 2005; Chen and Rong, 2009). obtained the solution formula applicable to the bearing capacity of the test specimen through experimental research and combined with the finite element simulation analysis. In (Liu, Y. M. 2012. Zhang, Xu and Zhao, 2010) studied the fire resistance of L-shaped concrete-filled steel tubular columns, and obtained the laws that the temperature of the fire-resistant surface of the test specimen under

the action of fire increased rapidly, the bearing capacity decreased significantly, and the fire back was relatively stable. In (Lin, Shen and Luo, 2009; Lei, Shen and Li, 2013) carried out an experiment on L-shaped concrete filled steel tubular members under low cyclic repeated load. The test results show that the ductility of the specimens decreased with the increase of axial compression ratio, and the increase of width to thickness ratio decreased the bearing capacity of the specimens.

In view of this new cross-section component, the related research at home and abroad is relatively lagging behind, and its basic theoretical system has not yet formed. However, the current research results are mainly concentrated in the short columns of special-shaped concrete-filled steel tubular columns, and some theoretical results have been preliminarily formed in the aspects of the ultimate bearing capacity and seismic performance of short columns. However, the research on the stability of medium and long columns of concrete-filled steel tube is still in its infancy. In this paper, the mechanical properties of L and T-shaped columns of concrete-filled steel tube are studied, and the simulation experiments of L and T-shaped concrete-filled steel tubular columns are carried out by using the finite element software ABAQUS. The main purpose of this paper is to analyze the influence of aspect ratio on the mechanical properties of L and T-shaped concrete-filled steel tubular columns, so as to provide theoretical basis for the practical application of the project and the research of subsequent scholars.

2 FINITE ELEMENT MODEL

2.1 Establishment of finite element model

For low-carbon steel and low-alloy steel, there are generally five stages of composition as shown in Figure 1 (a) during the uniaxial tension: elasticit oa , elastoplasticity ab ; plasticity bc , intensigy cd and necking de . In order to facilitate calculation, derivation and application, the strengthening and necking stage of steel are simplified as straight-line segment and introduced into the finite element software, and the mechanical properties are analyzed. The high-strength steel adopts the double fold load deformation curve of elastic and strengthening section as shown in Figure 1(b), in which the modulus of strengthening part is taken as 0.01es (Han, L. H.,2007)

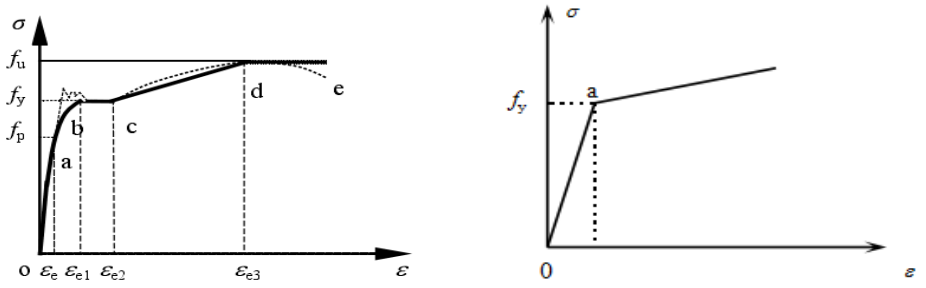

(a) Low-carbon steel (b) high-strength steel

Figure 1. Relation curve of steel

The paper combines the expression of constraint effect coefficient put forward by (Liu, W. and Han, L. H., 2006) at the same time, the modified equivalent stress-strain model expression of core concrete by Dr. Liu Wei of Fuzhou University is introduced as the constitutive model of concrete in the study of L and T-shaped CFST.

$$\sigma_0 = f_c(N/mm^2);\ \varepsilon_0 = \varepsilon_c + 800\cdot\xi^{0.2}\cdot 10^{-6};$$

$$\varepsilon_c = (1300 + 12.5\cdot f_c)\cdot 10^{-6};$$

The core concrete adopts three dimensional solid hexahedron elements C3D8R. Steel tube is defined as shell element S4, that is, four-node reduced integral shell element. The base plate with larger "width to thickness ratio" at both ends of the combined structure is set as rigid body. The mesh also adopts S4 unit. In this paper, a reasonable mesh size is obtained by comparing the test and calculation results of related literatures, which ensures that the simulation results remain within a reasonable error range. Fig. 2 and Fig. 3 are the cross-section mesh of L and T-shaped CFST columns for model verification and analysis.

In this paper, the model proposed by (Lu, X., et al, 2007) from Tongji University are selected to

simulate, analyze and verify the test data of L and T-shaped CFST columns.

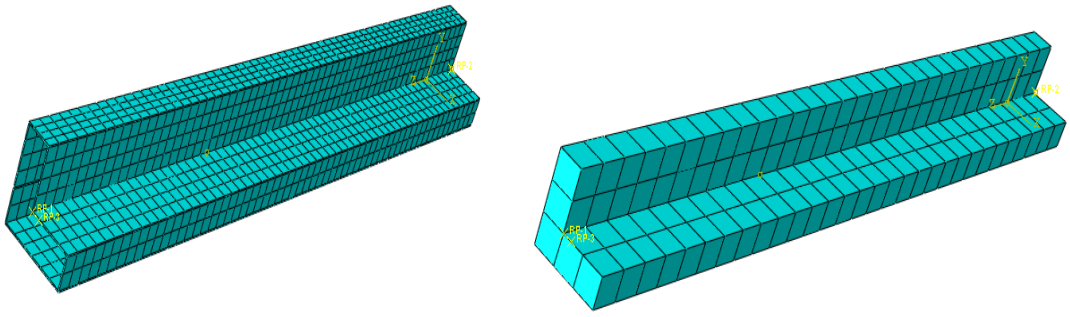

(a)Mesh generation of steel tube (b)Mesh generation of concrete

Fig. 2 Mesh generation of L-shaped CFST

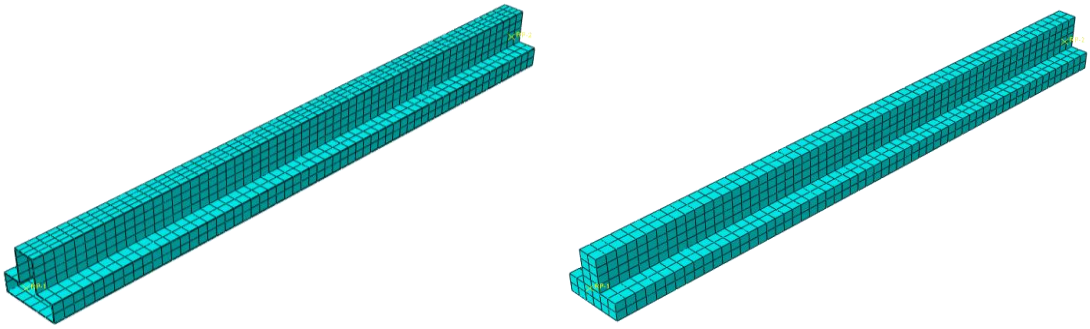

(a)Mesh generation of steel tube (b) Mesh generation of concrete

Fig. 3 Mesh generation of T-shaped CFST

2.2 Parameter design of test specimen

In this paper, the parameters of column size shown in Table 1 are selected as the test specimen for ABAQUS simulation analysis. The thickness and length of limbs in the section form of T and L-shaped CFST columns with equal limbs are 300mmand and 300 mm respectively. The column height of the test piece is 3000mm, 6000mm, 9000mm and 12000mm respectively; meanwhile, steel plates with 10 mm thickness and 300 mm length and width are respectively wrapped on the upper and lower column heads respectively to prevent the local damage of the test specimen from adverse impact on the test results. The steel performance parameters and test specimen parameters to be simulated are shown in Table 1 and Table 2 respectively.

Table 1. steel parameters

Steel tube thickness /mm	Modulus of elasticity $E_s/(N/mm^2)$	Yield strength f_y/MPa	Ultimate strength f_u/MPa	Poisson ratio
5	1.98×10^5	242	347	0.3

Table 2. Design parameters of test specimens with different aspect ratio

Sections	Specimens	Strength grade of concrete	Wall thickness of steel tube (steel ratio)	Specimen height /mm (aspect ratio)
Specimen L	L10	C40	5(0.123)	3000(10)
	L20	C40	5(0.123)	6000(20)
	L30	C40	5(0.123)	9000(30)
	L40	C40	5(0.123)	12000(40)
Specimen T	T10	C40	5(0.123)	3000(10)
	T20	C40	5(0.123)	6000(20)
	T30	C40	5(0.123)	9000(30)
	T40	C40	5(0.123)	12000(40)

2.3 Model validation

Comparing the test results of references with the results of finite element simulation, Table 3 shows the bearing capacity calculated by ABAQUS and test respectively. It can be seen that the error ratio between the simulated ultimate bearing capacity and the test bearing capacity is within 10%, and the error is within the acceptable range. Thus it shows the rationality of the finite element modeling method in this paper. To different incremental steps is shown respectively.

Table 3.Comparison of bearing capacity of test specimen

Specimens	Test bearing capacity (KN)	Simulated bearing capacity (KN)	Error ratio between test value and simulation value (%)
L-X1	3708	4019	8.4
L-X2	437	464	6.18
T-Y1	510	539	5.8

3 RESULTS OF FINITE ELEMENT ANALYSIS

3.1 Analysis of the influence of aspect ratio on the linear buckling of specimens

In order to study the critical load failure modes of L and T-shaped CFST columns subjected to eigenvalue buckling under different aspect ratios, the stress distribution map corresponding to the fourth-order eigenvalue of linear buckling is extracted for analysis. As shown in Figure 4-7 and Figure 8-11, the stress distribution of L and T-shaped specimen buckling modes corresponding only the distribution proportion of stress area in the specimen is different. When the first and second order eigenvalues of the specimen are damaged, the area where the material reaches the larger bearing capacity is smaller, and the utilization of the material is insufficient. When the specimen is in the third or fourth orders eigenvalue failure mode, the yield strength area of the specimen increases significantly, and the mechanical properties of the material play a more effective role (Pacurar; Balc and Berce et al. 2008).

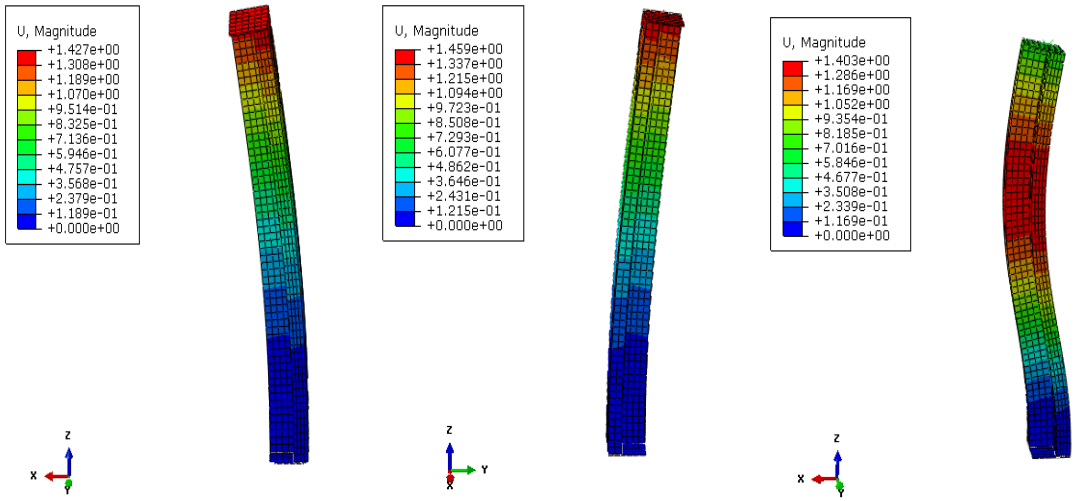

First order eigenvalue of L10 Second order eigenvalue of L10 Third order eigenvalue of L10

Fig. 4 Fourth-order buckling mode of L10

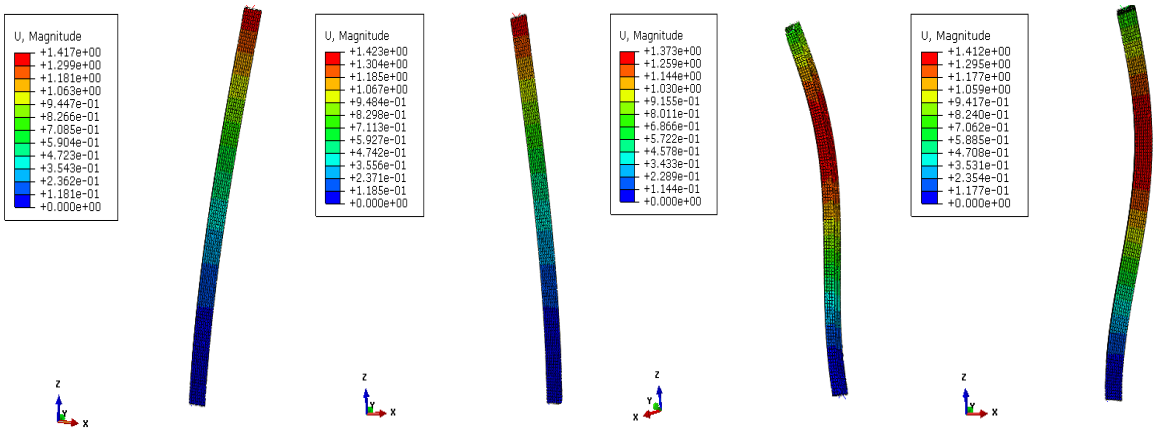

First order eigenvalue of L20 Second order eigenvalue of L20 Third order eigenvalue of L20 Fourth order eigenvalue of L20

Fig. 5 Fourth-order buckling mode of L20

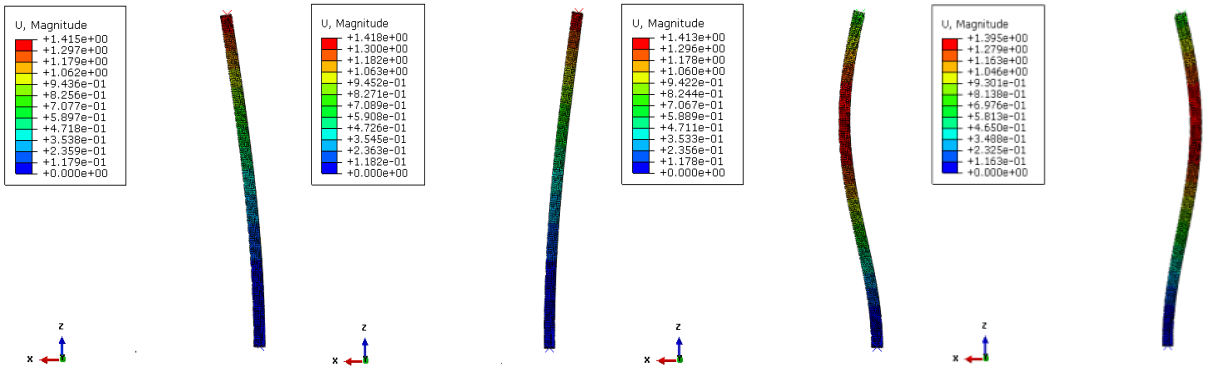

First order eigenvalue of L30 Second order eigenvalue of L30 Third order eigenvalue of L30 Fourth order eigenvalue of L30

Fig. 6 Fourth-order buckling mode of L30

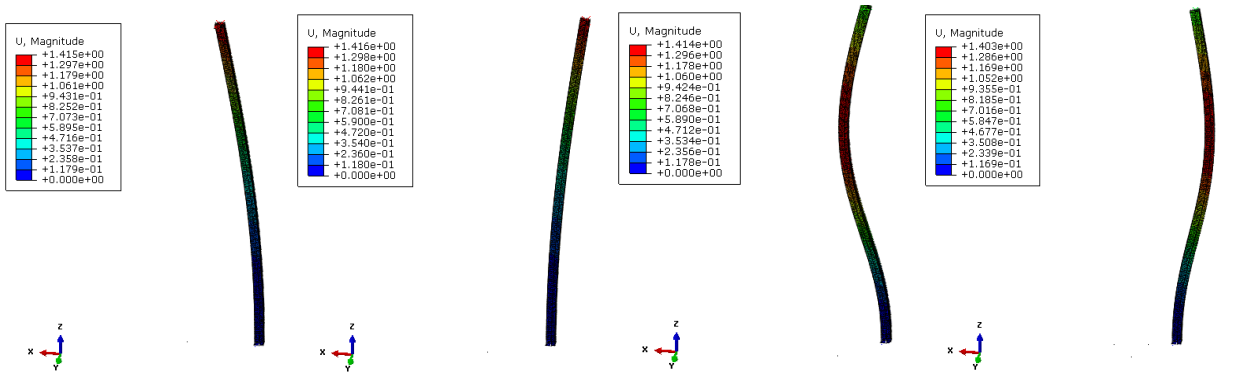

First order eigenvalue of L40 Second order eigenvalue of L40 Third order eigenvalue of L40 Fourth order eigenvalue of L40

Fig. 7 Fourth-order buckling mode of L40

From Figure 4-7, it can be seen that with the increase of aspect ratio of L-shaped specimen, the increment steps of eigenvalue buckling modes of it decrease gradually. It indicates that the linear buckling critical load of L-shaped specimen decreases with the increase of aspect ratio, and the trend is very obvious. However, the increase of aspect ratio has little effect on the shape of the eigenvector corresponding to the fourth-order eigenvalue of L-shaped specimen, and the distribution and change rule of stress are similar Pacurar and Berce, 2013).

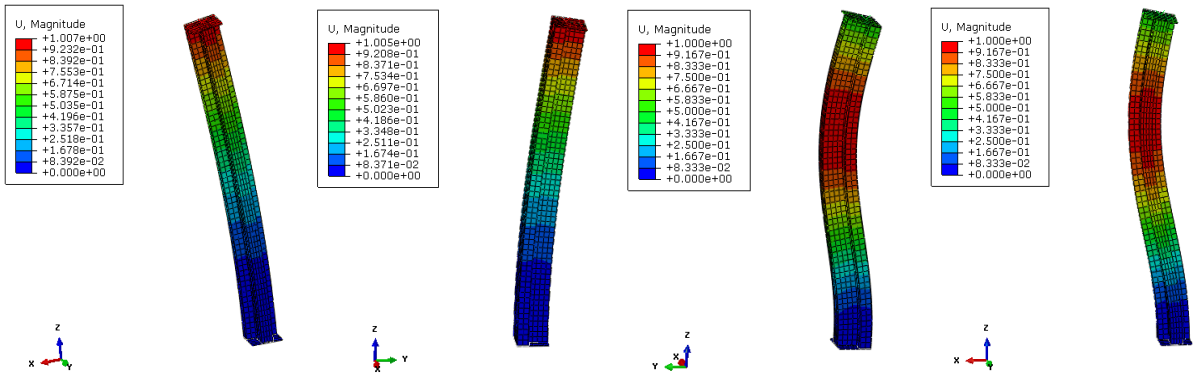

First order eigenvalue of T10 Second order eigenvalue of T10 Third order eigenvalue of T10 Fourth order eigenvalue of T10

Fig. 8 Fourth-order buckling mode of T10

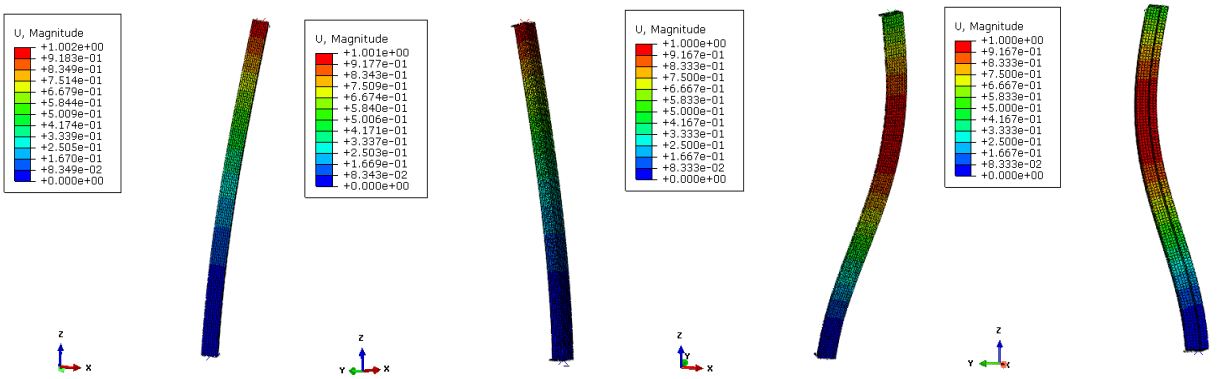

First order eigenvalue of T20 Second order eigenvalue of T20 Third order eigenvalue of T20 Fourth order eigenvalue of T20

Figure. 9 Fourth order buckling mode of T20

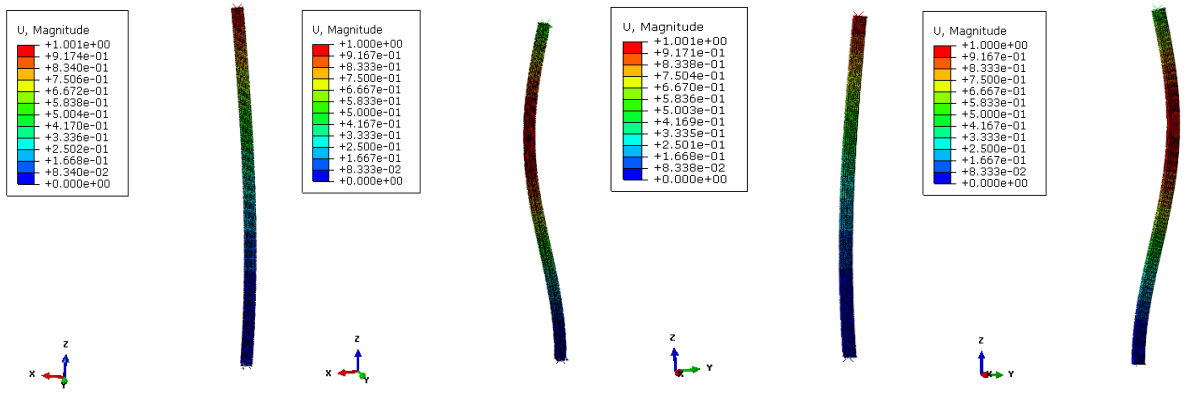

First order eigenvalue of T30 Second order eigenvalue of T30 Third order eigenvalue of T30 Fourth order eigenvalue of T30

Figure. 10 Fourth order buckling mode of T30

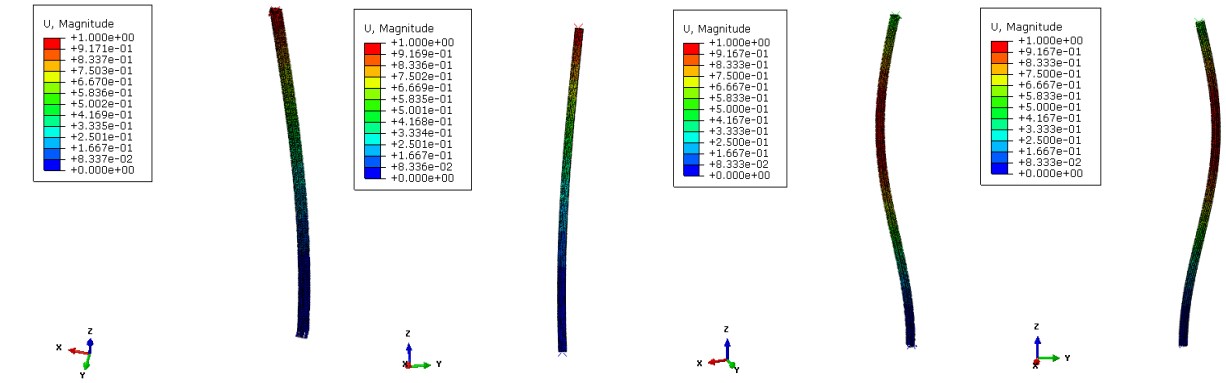

First order eigenvalue of T40 Second order eigenvalue of T40 Third order eigenvalue of T40 Fourth order eigenvalue of T40

Figure. 11 Fourth order buckling mode of T40

Figure 8-11 are the corresponding buckling modes of eigenvalues of T-shaped specimens under different aspect ratios. Through the above figures, it is found that the modal changes of each order eigenvalue of T-shaped specimen with different aspect ratios are basically the same. With the increase of aspect ratio, the proportion of the maximum yield stress area decreases when the specimen reaches the critical load. The increase of aspect ratio leads to the sharp increase of the increment step corresponding to the buckling of eigenvalues, which shows that the aspect ratio has a significant effect on the bearing capacity of T-shaped specimen.

In order to study the change rule of eigenvalue buckling critical load of L and T-shaped specimens under the action of different concrete strengths, the relevant data are extracted as shown in Table 4 and Table 5.

Table 4. Linear buckling critical load of L-shaped specimen

Specimens	Aspect ratio	Critical load /KN	Increase range of critical load /%
L10	10	3093.9	266.45
L20	20	844.29	124.75
L30	30	375.65	77.68
L40	40	211.42	-

Table 5. Linear buckling critical load of T-shaped specimen

Specimens	Aspect ratio	Critical load/KN	Increase range of critical load/%
T10	10	4585.60	297.47
T20	20	1153.70	124.65
T30	30	513.55	77.72
T40	40	288.96	-

From Table 4, when the aspect ratio reduced from 40 to 30, the critical load of L-shaped specimen increased by 77.68%. When it reduces from 30 to 20, the critical load of L-shaped specimen increases by 124.75%, and when it reduces from 20 to 10, the critical load of L-shaped specimen increases by 266.45%.

According to Table 5, when the aspect ratio reduces from 40 to 30, the critical load of T-shaped specimen increases by 77.72%; when it reduces from 30 to 20, the critical load of L-shaped specimen increases by 124.65%; and when it reduces from 20 to 10, the critical load of L-shaped specimen increases by 297.47%.

The above shows that with the decrease of aspect ratio, the critical load of L and T-shaped specimen increases more and more; that is, the aspect ratio plays a key role in the control of the bearing capacity of L and T-shaped CFST columns.

3.2 Analysis of the influence of aspect ratio on nonlinear buckling of specimens

Under the static load, in order to study the whole process of nonlinear load displacement change of T and L-shaped CFST columns with different aspect ratios, the drawing is shown in Fig. 12 and Fig. 13.

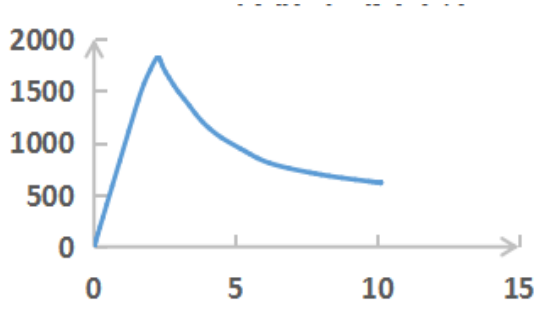

Load displacement curve of L10

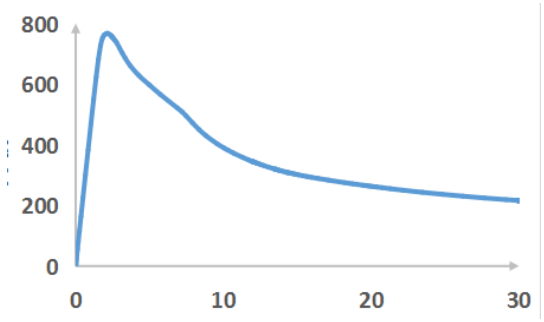

Load displacement curve of L20

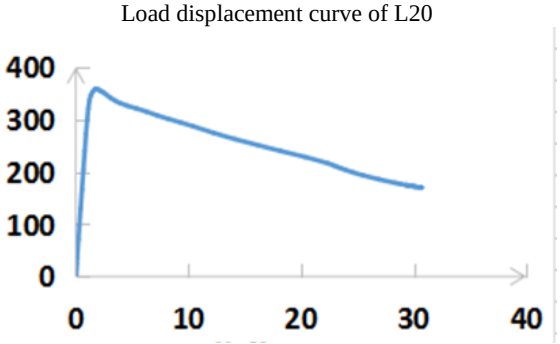

Load displacement curve of L30

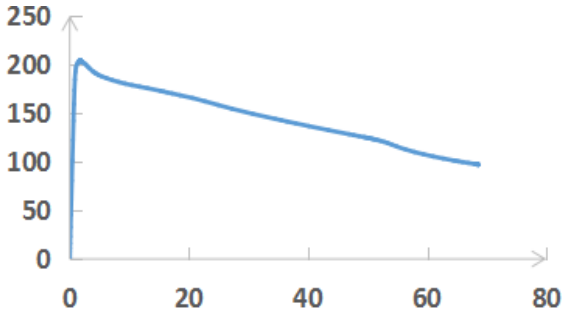

Load displacement curve of L40

Note: In the above four drawings, the abscissa is the displacement with unit mm; the ordinate is the composite with unit kn.

Figure 12. Load displacement curve of group L

As shown in Figure 12, when the aspect ratio of L-shaped specimen is 10, the load increases rapidly in the elastic deformation stage; When the critical load reaches, the vertical load drops sharply with the increase of the vertical displacement of the specimen, and the decrease of the load slows down with the increase of the displacement; When the displacement reaches about 5mm, the slope of the load with the displacement begins to ease. When the aspect ratio of the specimen is 20, the decreasing trend of the slope is about 10 mm. When the aspect ratio of the specimen continues to increase to 30 and 40, the load suddenly drops sharply after the specimen experiences elastic deformation and reaches the critical load. When the specimen is stable, the slope of load drop basically assumes a constant value with the increase of displacement.

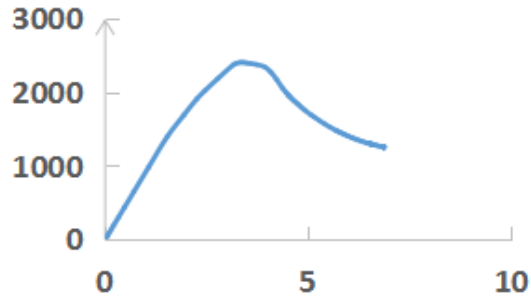

Load displacement curve of T10

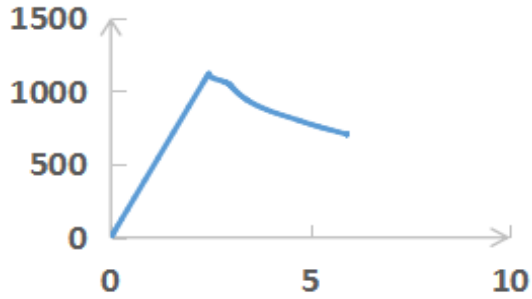

Load displacement curve of T20

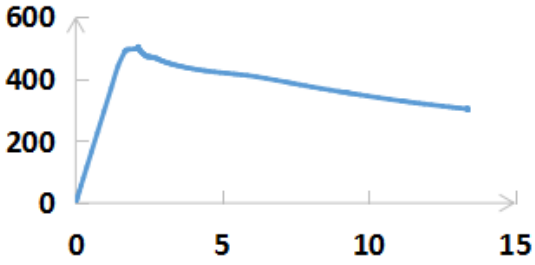

Load displacement curve of T30

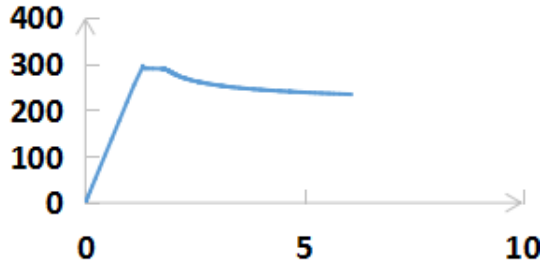

Load displacement curve of T40

Note: In the above four figures, the abscissa is the displacement with unit mm; the ordinate is the composite with unit kn.

Figure 13.Load displacement curve of group T

As shown in Figure 13, when the aspect ratio of T-shaped specimen is about 10, the growth slope of the load displacement curve is constant before the specimen reaches the critical load; that is, the specimen is in the elastic stage. When the critical load reaches, the slope of the decrease of the vertical load becomes larger and larger with the increase of the vertical displacement of the test specimen. When the displacement increases to about 5mm, the load decrease curve of the test specimen appears a turning point, and the

decrease of the bearing capacity becomes gentler and gentler. When the aspect ratio increases to 20, the slope of load decrease becomes more stable in the stage of elastic-plastic deformation. With the increase of the aspect ratio, the load drop rate of the specimen is lower and lower in the stage of instability.

3.3 Comparative analysis of bearing capacity of L and T-shaped specimens with different aspect ratios

In order to obtain the quantitative rule of the non-eigenvalue buckling critical load change of L and T-shaped specimens under the action of different aspect ratios, the comparison of the critical load values is shown in Table 6 and Table 7 respectively.

Table 6. Nonlinear buckling critical load of L-shaped specimen

Specimens	Aspect ratio	Critical load/KN	Increase range of critical load /%
L10	10	1815.98	136.55
L20	20	767.68	114.29
L30	30	358.25	75.81
L40	40	203.77	-

Table 7. Nonlinear buckling critical load of T-shaped specimen

Specimens	Aspect ratio	Critical load/KN	Increase range of critical load /%
T10	10	2602.68	133.03
T20	20	1116.89	125.02
T30	30	496.35	80.33
T40	40	275.25	-

According to Table 6, when the aspect ratio of L-shaped specimen reduces from 40 to 30, the critical load of L-shaped specimen increases by 75.81%; when it reduces from 30 to 20, the critical load of L-shaped specimen increases by 114.29%; and when it reduces from 20 to 10, the critical load of L-shaped specimen increases by 136.55%.

According to Table 7, when the aspect ratio of L-shaped specimen reduces from 40 to 30, the critical load of T-shaped specimen increases by 80.33%; when it reduces from 30 to 20, the critical load of T-shaped specimen increases by 125.02%; and when it reduces from 20 to 10, the critical load of T-shaped specimen increases by 133.03%.

It shows that with the decrease of aspect ratio, the critical load of L and T-shaped specimens increases more and more. That is, if the aspect ratio increases, the critical load of nonlinear buckling of specimens will decrease exponentially. In engineering application, it is very important to coordinate the relationship between the bearing capacity and the aspect ratio.

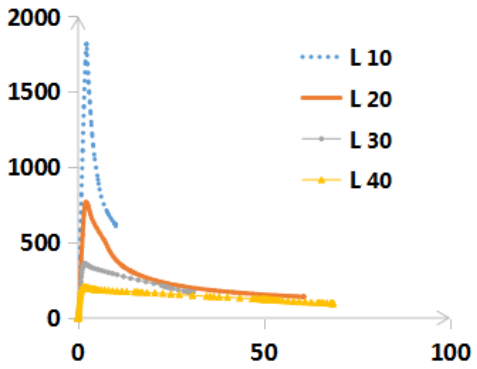

Figure 14. Comparison of load displacement curve of group L

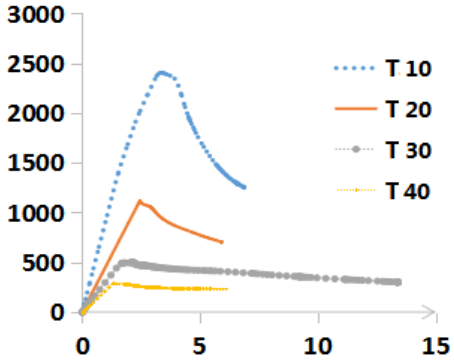

Figure 15. Comparison of load displacement curve of group T

Note: In the above two figures, the abscissa is the displacement with unit mm; the ordinate is the composite with unit kn.

As shown in Fig. 14 and Fig. 15, the load displacement curves of the corresponding L and T groups of specimens are compared. It is shown that with the increase of aspect ratio, the critical load value of L and T-shaped specimens is decreasing; in the elastic-plastic stage, the load curve slows down with the displacement after the deformation reaches a certain stage generally; the T-shaped specimen is more obvious than the L-shaped specimen. It shows that with the increase of aspect ratio, the bearing capacity of the specimen is decreasing greatly, while the ductility of the specimen in the stage of elastic-plastic failure is increasing correspondingly.

4 CONCLUSION

In this paper, the influence of aspect ratio on the mechanical properties of L and T-shaped CFST middle and long columns is analyzed by using the finite element simulation. The following rules are obtained:

(1) The aspect ratio plays a key role in the control of the bearing capacity of L and T-shaped CFST columns. With the decrease of aspect ratio, the critical load of L and T-shaped specimens increases exponentially.

(2)With the increase of aspect ratio, the critical load of L and T-shaped specimens shows a downward trend, while the displacement of specimens when they reach the critical load decreases gradually and the ductility of specimens increase correspondingly.

(3)In the elastic deformation stage, the curve growth rate decreases with the increase of aspect ratio; in the elastic-plastic stage, the load curve slows down with the displacement after the deformation reaches a certain stage generally; T-shaped specimen is more obvious than L-shaped specimen.

(4)The failure of T-shaped concrete-filled steel tubular columns is more manifested in the out of control stability, resulting in excessive deformation and withdrawal from the working mechanism. Controlling the aspect ratio of specimen is the necessary foundation for the effective utilization of medium and long special concrete-filled steel tubular columns. Therefore, the study of the influence of aspect ratio on the mechanical properties of special-shaped concrete-filled steel tubular columns should be strengthened. Therefore, the bearing capacity of L and T-shaped specimens can be improved by limiting the aspect ratio in engineering design.

REFERENCES

► Chen, Z. H. and Rong, B. (2009), Research on axinl compression stability of L-shaped column composed of concrete filled square steel tubes, *Building Structure*, vol.6, pp. 39-42+33.

► Han, L. H. (2007), Theory and practice of CFST structure, *Beijing: Science Press.*

► Hu, H.T., Huang, C.S., Wu, M.H. and Wu, Y.M. (2003), Nonlinear Analysis of Axially Loaded Concrete-Filled Tube Columns with Confinement Effect, *Journal of Structural Engineering*, vol. 129 no. 10, pp. 1322-1329.

► Lei, M., Shen, Z. Y. and Li, Y. Q. (2013). Research status of special-shaped concrete-filled steel tubular columns, Structural *engineer*. Vol. 3, pp. 155-163.

► Lin, Z. Y, Shen, Z. Y. and Luo, J. H. (2009), Hysteretic Behavior of Concrete-Filled L-Section Steel Tubular Columns under Cyclic Loading", *Progress in Steel Building Structures*, vol. 11 no. 02, pp. 12-17.

► Liu, W. and Han, L. H. (2006), Behaviors of concrete-filled steel tubes subject axial local compression, *China Civil Engineering Journal*, vol. 39 no. 6, pp. 19-27.

► Liu, Y. M. (2012), Temperature field analysis of L-shaped concrete-filled steel tube core column, *Concrete*, vol. 5, pp. 138-140.

► Lu, X., Li, X., & Wang, D. (2007), Modelling and experimental verification on concrete-filled steel tubular columns with L or T section, *Frontiers of Architecture and Civil Engineering in China*, vol. 1 no. 2, pp. 163-169.

► Pacurar, Razvan; Balc, Nicolae; Berce, Petru; et al. (2008). *Research on improving the mechanical properties of the sls metal parts, rapid prototyping* Journal Conference: 19th International Symposium of the Danube Adria Association for Automation and Manufacturing Location: Trnava, SLOVAKIA Date: OCT 22-25, 2008. Pages: 1003-1004

► Pacurar, Razvan; Berce, Petru (2013). *Research on the durability of injection molding tools made by selective laser sintering technology, Proceedings of the romanian academy series a-mathematics physics technical sciences information science* volume: 14 issue:3, pages: 234-241. published: Jul-Sep, 2013

► Rong, B. and Chen, Z. H. (2005), Analysis of the calculation method of square and rectangular CFST columns based on superposition theory", *Tianjing University. Proceedings of the Fifth National Symposium on modern structural engineerin*, vol. 5.

► Shanmugam, N. E., Lakshmi, B. and Uy, B. (2002), An analytical model for thin-walled steel box columns with concrete in-fill, *Engineering Structures*, vol. 24 no. 6, pp. 825–838.

► Uy B. (2001), Local and Post local Buckling of Fabricated Steel and Composite Cross ections, *Journal of Structural Engineering*, vol. 127 no. 6, pp. 666-677.

► Uy, B. (2000), Strength of Concrete Filled Steel Box Columns Incorporating Local Buckling, *Journal of Structural Engineering*, vol. 126 no. 3, pp. 341-352.

► Uy, B. (2001), Strength of short concrete filled high strength steel box columns, *Journal of Constructional Steel Research*, vol. 57 no. 2, pp. 113-134.

► Wang, D. (2005) Experimental study on seismic behavior of T-shaped and L-shaped CFST columns, *A report on the postdoctoral research of Tongji University.*

► Wang, D., LV, X. L. (2005), Experimental study on seismic behavior of concrete-filled steel T-section and L-section columns, *Journal of Building Structures*, vol. 26 no. 4, pp. 39-44+106.

► Zhang, Y. B., Xu, Y. F. and Zhao, X. (2010), Analysis of the fire resistance limit of L-shaped concrete filled steel tubular core columns under different loads, *Scientific and technological innovation and industrial development (volume A) -Proceedings of the 7th Shenyang annual conference of science and technology and the collection of papers of Hunnan high tech Industrial Development Forum*, vol. 5.